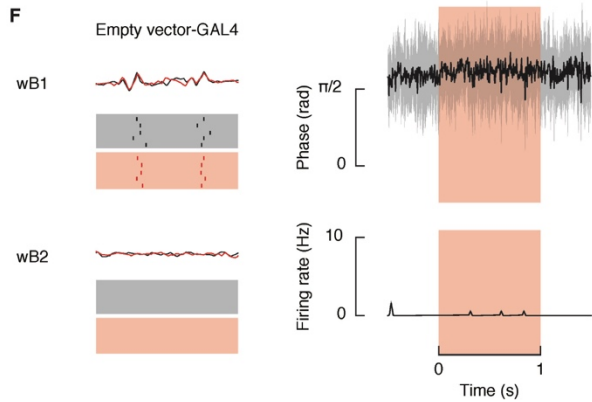
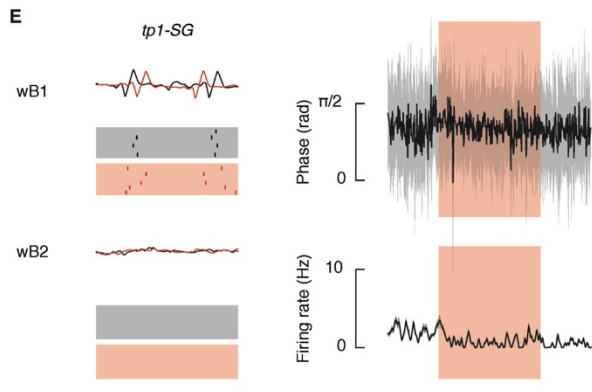
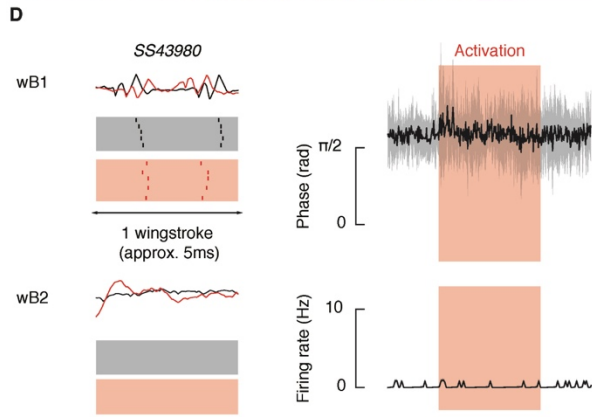
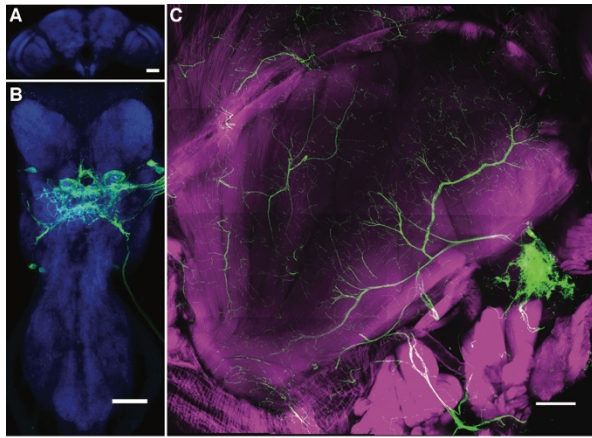


**Figure S1. Haltere muscle tuning dynamics about the yaw-roll and pitch-roll axes. Related to Figure 1.** (A and B) Direction of stimulus (arrows) with wing beat amplitude responses and fluorescent signals in basalar and axillary muscles in response to 3 second presentations of wide-field motion where the center of rotation shifted in 30° increments about the yaw-roll (A) or pitch-roll (B) plane. Stimulus direction follows the right-hand rule. Data shown represent mean  $\pm$  95% CI ( $n = 15$  flies each).



**Figure S2. Activation of wing power muscle motor neurons. Related to Figure 4.** (A and B) Maximum intensity projections of the brain (A) and ventral nerve cord (B) showing GFP expression driven by *SS43980-GAL4*. The wing power muscle motor neurons are in the mesothoracic segment of the VNC. Blue channel shows nc-82 staining. (C) *SS43980-GAL4* labels the dorsolongitudinal and dorsoventral wing muscle motor neurons. Magenta channel shows phalloidin staining of muscle. For anatomy of *tp1-SG*, see [S1]. Scale bars: 50 $\mu$ m (A, B); 100  $\mu$ m (C). (D to F) Left: Example muscle action potentials and rasters of wB1 and wB2 before (black) and after (red) optogenetic activation of *SS43980-GAL4* (D), *tp1-SG* (E), and *empty vector-GAL4*. Rasters similar to those in Fig. 4. Right: Instantaneous wB1 phase or wB2 firing rate of each driver line in response to optogenetic activation. Data shown represent circular mean  $\pm$  circular STD,  $n = 8$  (D, wB1); 5 (D, wB2); 6 (E, wB1); 4 (E, wB2), 7 (F, wB1); 5 (F, wB2).

### Supplemental References

S1. O'Sullivan, A., Lindsay, T., Prudnikova, A., Erdi, B., Dickinson, M., and von Philipsborn, A.C. (2018). Multifunctional wing motor control of song and flight. *Curr. Biol.* 28, 2705-2717.